Upconversion ultraviolet random lasing in Nd^{3+} doped fluoroindate glass powder

Marcos A. S. de Oliveira,[1] Cid B. de Araújo,[1,*] and Younes Messaddeq[2]

[1]*Departamento de Física, Universidade Federal de Pernambuco, 50670-901 Recife, PE, Brazil*
[2]*Instituto de Química, Universidade do Estado de São Paulo, 14801-970 Araraquara, SP, Brazil*
**cid@df.ufpe.br*

Abstract: An upconversion random laser (RL) operating in the ultraviolet is reported for Nd^{3+} doped fluoroindate glass powder pumped at 575 nm. The RL is obtained by the resonant excitation of the Nd^{3+} state $^2G_{7/2}$ followed by energy transfer among two excited ions such that one ion in the pair decays to a lower energy state and the other is promoted to state $^4D_{7/2}$ from where it decays emitting light at 381 nm. The RL threshold of 30 kW/cm^2 was determined by monitoring the photoluminescence intensity as a function of the pump laser intensity. The RL pulses have time duration of 29 ns that is 50 times smaller than the decay time of the upconversion signal when the sample is pumped with intensities below the RL laser threshold.

OCIS codes: (190.0190) Nonlinear optics; (140.3530) Lasers, neodymium; (140.5680) Rare earth and transition metal solid-state lasers; (140.3613) Lasers, upconversion; (140.3610) Lasers, ultraviolet.

References and links

1. H. Cao, "Lasing in random media," Waves Random Media **13**(3), R1–R39 (2003).
2. M. A. Noginov, *Solid-State Random Lasers* (Springer, 2005).
3. D. S. Wiersma, "The physics and applications of random lasers," Nat. Phys. **4**(5), 359–367 (2008).
4. D. S. Wiersma and M. A. Noginov, "Nano and random lasers," J. Opt. **12**(2), 020201–024014 (2010).
5. N. M. Lawandy, R. M. Balachandran, A. S. L. Gomes, and E. Sauvain, "Laser action in strongly scattering media," Nature **368**(6470), 436–438 (1994).
6. H. Cao, Y. G. Zhao, H. C. Ong, S. T. Ho, J. Y. Dai, J. Y. Wu, and R. P. H. Chang, "Ultraviolet lasing in resonator forward by scattering in semiconductor polycrystalline films," Appl. Phys. Lett. **73**(25), 3656–3658 (1998).
7. X. Meng, K. Fujita, S. Murai, and K. Tanaka, "Coherent random lasers in weakly scattering polymer films containing silver nanoparticles," Phys. Rev. A **79**(5), 053817 (2009).
8. A. M. Brito-Silva, A. Galembeck, A. S. L. Gomes, A. J. Jesus-Silva, and C. B. de Araújo, "Random laser action in dye solutions containing Stöber silica nanoparticles," J. Appl. Phys. **108**(3), 033508 (2010).
9. B. Li, G. Williams, S. C. Rand, T. Hinklin, and R. M. Laine, "Continuous-wave ultraviolet laser action in strongly scattering Nd-doped alumina," Opt. Lett. **27**(6), 394–396 (2002).
10. S. M. Redmond, G. L. Armstrong, H.-Y. Chan, E. Mattson, A. Mock, B. Li, J. R. Potts, M. Cui, S. C. Rand, S. L. Oliveira, J. Marchal, T. Hinklin, and R. M. Laine, "Electrical generation of stationary light in random scattering media," J. Opt. Soc. Am. B **21**(1), 214–222 (2004).
11. H. Fujiwara and K. Sasaki, "Observation of upconversion lasing within a thulium-ion-doped glass powder film containing titanium dioxide particles," Jpn. J. Appl. Phys. **43**(No. 10B), L1337–L1339 (2004).
12. M. A. R. C. Alencar, A. S. L. Gomes, and C. B. de Araújo, "Directional laserlike emission from a dye-doped polymer containing rutile nanoparticles," J. Opt. Soc. Am. B **20**(3), 564–567 (2003).
13. C. J. S. de Matos, L. de S Menezes, A. M. Brito-Silva, M. A. Martinez Gámez, A. S. L. Gomes, and C. B. de Araújo, "Random fiber laser," Phys. Rev. Lett. **99**(15), 153903 (2007).
14. Q. Song, L. Liu, and L. Xu, "Directional random-laser emission from Bragg gratings with irregular perturbation," Opt. Lett. **34**(3), 344–346 (2009).
15. M. Gagné and R. Kashyap, "Demonstration of a 3 mW threshold Er-doped random fiber laser based on a unique fiber Bragg grating," Opt. Express **17**(21), 19067–19074 (2009).
16. E. Pecoraro, S. García-Revilla, R. A. S. Ferreira, R. Balda, L. D. Carlos, and J. Fernández, "Real time random laser properties of Rhodamine-doped di-ureasil hybrids," Opt. Express **18**(7), 7470–7478 (2010).
17. C. B. de Araújo, G. S. Maciel, L. de S. Menezes, N. Rakov, E. L. Falcão-Filho, V. A. Jerez, and Y. Messaddeq, "Frequency upconversion in rare-earth doped fluoroindate glasses," C. R. Chim. **5**(12), 885–898 (2002).

#142058 - $15.00 USD Received 3 Feb 2011; revised 28 Feb 2011; accepted 28 Feb 2011; published 10 Mar 2011

18. E. L. Falcão-Filho, C. B. de Araújo, and Y. Messaddeq, "Frequency upconversion involving triads and quartets of íons in a Pr^{3+} / Nd^{3+} codoped fluoroindate glass," J. Appl. Phys. **92**(6), 3065–3070 (2002).
19. L. de S. Menezes, C. B. de Araújo, Y. Messaddeq, and M. A. Aegerter, "Frequency upconversion in Nd^{3+} doped fluoroindate glass," J. Non-Cryst. Solids **213–214**, 256–260 (1997).
20. G. S. Maciel, L. de S. Menezes, C. B. de Araújo, and Y. Messaddeq, "Violet and blue light amplification in Nd3+ doped fluoroindate glasses," J. Appl. Phys. **85**, 6782–6785 (1999).
21. M. Yamane and Y. Asahara, *Glasses for Photonics* (Cambridge University Press, 2000).

1. Introduction

The subject of random lasers (RLs) is receiving large attention due to the unique properties of RLs and to their potential applications [1–16]. Generation of laserlike emission from strongly scattering media has been observed and studied in a large variety of systems such as dye solutions containing scattering particles, semiconductor powders, polymers, and nanoparticles doped with rare-earth (RE) ions.

There are two main classes of RLs: one in which passive scatterers are embedded in a gain medium (such as TiO_2 nanoparticles suspended in a colloid containing dye molecules [5]) and another class in which the scatterers are active (such as ZnO nanorods arrays [6]). The RL action may occur when there is an excitation threshold, due to the multiple scattering, above which the total optical gain is larger than the losses. Optical modes with a central frequency, narrow bandwidth, short lifetime and a complex spatial profile are defined by the scattering process [3].

The first RL based on a Nd^{3+} doped powder was reported in 1986 [2]. Crystalline particles with dimensions from 1 to 10 μm were excited by a dye laser operating in the orange-red region and RL emission was obtained at 1.06 μm. The experiment was made at 77 K and the laser threshold was ≈600 kW/cm^2. More recently Nd^{3+} nanocrystals have been investigated and the mechanisms of excitation and relaxation participating in the process were studied. A list of more than 30 materials doped with Nd^{3+} as well as many reports based on other RE ions are given in Ref. [2]. It was observed that the maximum efficiency is obtained for particles with dimensions between 1 and 100 μm. In the blue region RL was obtained for Nd^{3+} doped alumina nanoparticles for excitation by electron beams with energy varying from 2 to 10 KeV [9,10].

Most of the optically pumped RLs reported for RE doped systems are based on Stokes processes, i.e.: the RL wavelength is larger than the pumping wavelength. RL based on an anti-Stokes process involving RE ions was reported only for Tm^{3+}-doped fluorozirconate glass powder containing micrometer size titanium dioxide particles excited with a laser operating at 1064 nm [11]. Frequency upconversion (UC) RL emission at 793 nm (450 nm) was observed with pump intensity threshold of 2.6 kW/cm^2 (6.3 kW/cm^2).

In the present paper we report on the operation of a UC random laser emitting at 381 nm obtained from a Nd^{3+} - doped glass powder pumped by a pulsed dye laser operating at 575 nm, in resonance with the Nd^{3+} transition $^4I_{9/2} \rightarrow {}^2G_{7/2}$. The RL threshold was 30 kW/cm^2 and RL pulses of 29 ns were observed for pumping above the threshold.

A fluoroindate glass (FIG) was used because it is a very efficient upconverter [17–20]. Besides the large UC efficiency and its capability to incorporate large concentration of RE ions into the matrix, FIG has high resistance to moisture, good chemical and mechanical stability, and large transparency window from 0.2 to 8 μm. UC processes due to energy transfer involving pairs, triads, and quartets of RE ions in FIG were studied under appropriate conditions for various RE ions [17–20]. In particular we refer to a previous experiment with Nd^{3+} doped FIG samples pumped at 577 nm that showed strong UC emission in the violet – blue region [19] and experiments where samples excited in the green – orange region showed large optical gain at 382 and 414 nm [20]. The gain measured when pumping with a laser beam near resonance with the Nd^{3+} transition $^4I_{9/2} \rightarrow {}^2G_{7/2}$ was four orders of magnitude larger than when the sample was excited at 532 nm.

#142058 - $15.00 USD Received 3 Feb 2011; revised 28 Feb 2011; accepted 28 Feb 2011; published 10 Mar 2011

2. Experimental details

Glass samples with compositions (in mol %) (41-x)InF_3-20ZnF_2-20SrF_2-16BaF_2-2NaF-1GaF_3-xNdF_3 (x = 0.5, 1.0, and 3.0) were fabricated. Standard pro-analysis oxides and fluorides were used as starting materials for the glass synthesis and the classical ammonium bifluoride process was employed [17]. The fluoride powders were mixed together and heat treated at 700 °C for melting and then 800 °C for refining. The melt was poured and cooled into a preheated mold. Finning, casting, and annealing were carried out under dry argon atmosphere and samples with good optical quality were obtained. Afterwards a powder with grains having average size between 25 and 38 μm (measured using an electron microscope) was prepared by crushing the glass samples and passing the grains through calibrated sieves. Finally the amorphous powder was gently pressed to a volume of ≈8 mm^3 using a sample-holder fabricated for the optical experiments.

The absorption spectra of the bulk samples were measured using a commercial spectrophotometer from the near-ultraviolet to the near-infrared. A dye laser using Rhodamine 590 dissolved in ethanol, pumped by the second harmonic of a pulsed Nd: YAG laser (532 nm, 8 ns, 5 Hz) was used as the excitation source. The dye laser beam was focused on the sample using a 20 cm focal length lens. The signal emitted by the sample was collected using a 5 cm focal length lens, along ≈45° direction with respect to the laser beam propagation direction. The luminescence spectrum was recorded through a 0.5 m monochromator followed by a photomultiplier coupled to a computer.

3. Results and discussion

Figure 1 shows the absorption spectrum of the bulk sample with x = 3.0. The features correspond to electronic transitions involving states in the 4*f* configuration, starting from the ground state ($^4I_{9/2}$) of the Nd^{3+} ions to the excited states labeled in the figure. The other samples present similar spectrum. The positions of the Nd^{3+} bands are independent of the concentration but their amplitudes are proportional to the Nd^{3+} concentration. The large bandwidths are due to the inhomogeneous broadening caused by the different crystalline fields in the various sites occupied by the Nd^{3+} ions.

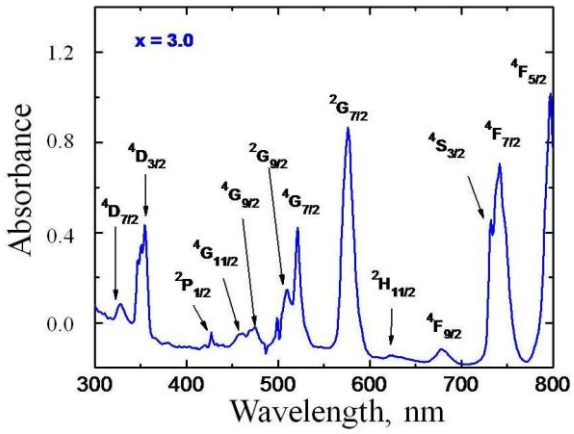

Fig. 1. Absorption spectrum of fluoroindate glass doped with Nd^{3+} ions. Sample length: 1.8 mm.

Figure 2 shows the luminescence spectrum of the powder samples for excitation at 575 nm in resonance with the transition $^4I_{9/2} \rightarrow {}^2G_{7/2}$. Other luminescence transitions were observed in other wavelengths but they are not relevant for the present experiment (the complete UC spectrum for the bulk sample was published in Ref. [19]). The spectra for the other powder samples present the same emission lines. For small excitation intensity the violet and blue

#142058 - $15.00 USD Received 3 Feb 2011; revised 28 Feb 2011; accepted 28 Feb 2011; published 10 Mar 2011

luminescence exhibited a quadratic dependence with the laser intensity indicating that two laser photons are necessary to generate each UC photon.

The UC lines in the 365 to 435 range were also reported for bulk samples in [20]. Gain parameters were determined for both spectral lines using a broad band incoherent light source as the probe beam at the spectral region of interest (~360–440 nm) and a pump beam at 583 or 532 nm. The emission at 381 nm was attributed to transitions $^4D_{7/2} \rightarrow {}^4I_{13/2}$

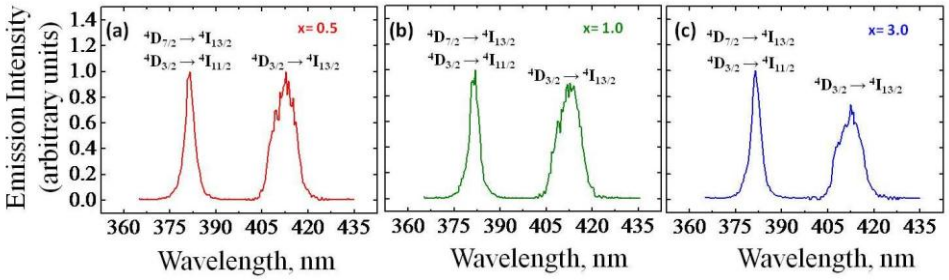

Fig. 2. Luminescence spectra in the wavelength range of interest. Excitation wavelength: 575 nm.

and $^4D_{3/2} \rightarrow {}^4I_{11/2}$ while the emission at 412 nm was attributed to the transition $^4D_{3/2} \rightarrow {}^4I_{13/2}$. The measured gain for the line at 381 nm for Nd^{3+} concentrations (x = 0.5, 1.0, and 3.0) assumed values between 30% and 100% larger than for the 412 nm line.

In the present experiments with FIG powders, the RL behavior was identified only for the emission at 381 nm and therefore the intensity behavior of the emission at 412 nm will not be discussed.

Although the UC light was emitted along a large solid angle, the signal recorded was contained in a small solid angle centered in the 45° direction with respect to the propagation of the pump laser. The intensity emitted did not change much for small angular deviations with respect to the direction of observation.

Figure 3(a) shows the dependence of the intensity at 381 nm as a function of the incident laser intensity for the sample with x = 3.0. A fast signal with ≈29 ns duration is observed for pump intensities of 40 and 50 kW/cm^2 followed by a long tail that extends for microseconds. For pump intensity of 20 kW/cm^2 only the slow signal, with the decay and rise times given in Table 1, is observed. Figure 3(b) shows the time evolution of the 381 nm signal for the three samples for pump intensity of 50 kW/cm^2. Figure 3(c) shows the UC lineshapes for pump at 575 nm and at 532 nm, with intensity of 50 kW/cm^2. The spectral

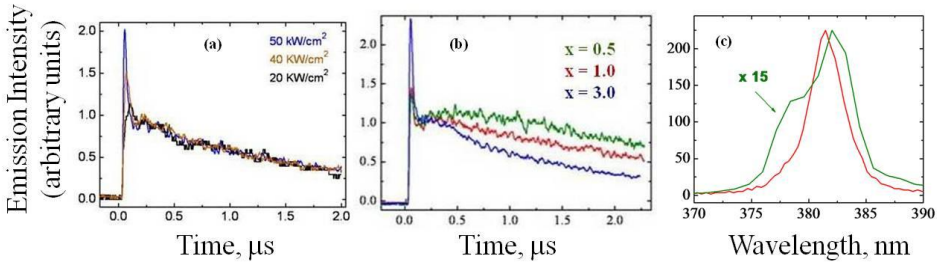

Fig. 3. (a) Intensity at 381 nm versus the input intensity at 575 nm (sample with x = 3.0). (b) Temporal evolution of the UC signal. Laser intensity: 50 kW/cm^2. (c) UC spectra for pumping at 575 nm (red line) and 532 nm (green line).

change is attributed to the signal amplification of a particular class of ions in the inhomogeneously broadened line.

#142058 - $15.00 USD Received 3 Feb 2011; revised 28 Feb 2011; accepted 28 Feb 2011; published 10 Mar 2011

Table 1. Decay and Rise Times of the 381 nm Signal for Pump Intensities Smaller Than 20 kW/cm^2, Obtained Through Fittings of the Function $f(t) \propto \left| e^{-t/t_1} - e^{-t/t_2} \right|$

	x = 0.5	x = 1.0	x = 3.0
Decay time, t_1	10.5 μs	6.6 μs	2.1μs
Rise time, t_2	0.2 μs	0.2 μs	0.03 μs

To analyze the results we first consider that two possible UC pathways may contribute for the results. From the energy level scheme of the Nd^{3+} ions, shown in Fig. 4(a), we observe that one possible pathway would start by one–photon absorption from the ground state to state $^2G_{7/2}$ followed by excited state absorption to states with energy of ≈34780 cm^{-1}.

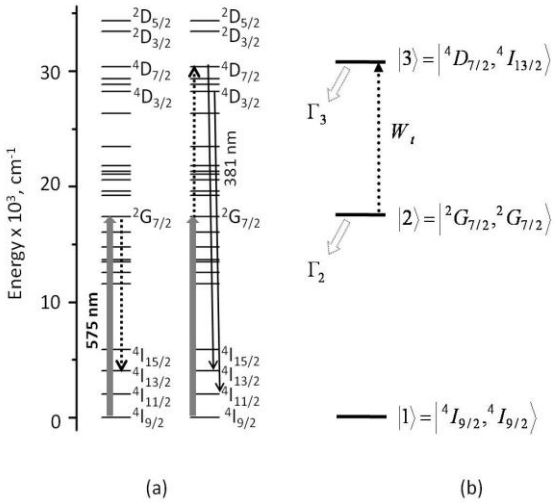

Fig. 4. (a) Simplified energy level scheme of Nd^{3+} ions with indication of the radiative transitions (solid lines) and the relevant energy transfer process (dashed lines). (b) Pair states involved in the UC process.

However this pathway is discarded because the UC intensity would vary linearly with the Nd^{3+} concentration. Hence, another UC pathway has to be considered because of the quadratic dependence of the 381 nm signal with the Nd^{3+} concentration and its dynamical behavior that presents a rise time slower than the laser pulse. We attribute the UC emission to energy transfer between excited Nd^{3+} ions. Accordingly, after resonant excitation of the Nd^{3+} ions to level $^2G_{7/2}$, pairs of coupled ions may exchange energy in such way that one ion is promoted to level $^4D_{7/2}$ while the other decays to level $^4I_{3/2}$. The cross–relaxation process ($^2G_{7/2,}$ $^2G_{7/2}$) → ($^4I_{13/2}$, $^4D_{7/2}$) is resonant being efficient and fast. Finally the ions at level $^4D_{7/2}$ may decay radiatively to level $^4I_{13/2}$ or, by nonradiative decay, they reach level $^4D_{3/2}$ from where they decay to level $^4I_{11/2}$ emitting at 381 nm. The equations describing the dynamics of the anti-Stokes signal are written considering the pair states indicated in Fig. 4(b) in the first approximation, neglecting mixing of individual ions' states due to the interaction potential. The population densities $N_2(t)$ and $N_3(t)$ of the pair states $|2\rangle$ and $|3\rangle$ satisfy the coupled equations

$$\frac{dN_2(t)}{dt} = -(\Gamma_2 + W_t) N_2(t), \qquad (1)$$

and

#142058 - $15.00 USD Received 3 Feb 2011; revised 28 Feb 2011; accepted 28 Feb 2011; published 10 Mar 2011

$$\frac{dN_3(t)}{dt} = W_t N_2(t) - \Gamma_3 N_3(t), \tag{2}$$

where $N_i(t)$ and Γ_i represent the population density and relaxation rate of state $|i\rangle$, $i = 1, 2$ and 3, respectively. W_t is the energy transfer rate between states $|2\rangle$ and $|3\rangle$. The population density of state $|3\rangle$ is given by

$$N_3(t) = \frac{W_t N_2(t)}{\Gamma_3 - (\Gamma_2 + W_t)} \left[e^{-(\Gamma_2 + W_t)t} - e^{-\Gamma_3 t} \right]. \tag{3}$$

The UC signal is proportional to $N_3(t)$ and can be compared to the experimental data for intensities smaller than 30 kW/cm^2.

The rise time of the 318 nm signal is due to the cross-relaxation rate between two excited Nd^{3+} ions at level $^2G_{7/2}$ that is a function of the Nd^{3+} ions concentration, and the time to populate level $^4D_{3/2}$ by nonradiative decay from level $^4D_{7/2}$. According to the *energy gap law* [21] the nonradiative relaxation rate is inversely related to the energy gap between two electronic states. Considering the cutoff phonon energy of the FIG matrix (≈500 cm^{-1}), we estimate that the level $^4D_{7/2}$ has lifetime of ≈22 ns. Also using the *energy gap law*, we estimate ≈4 μs for the lifetime of level $^4D_{3/2}$. Then, considering the slow UC decay for low pump intensity, we concluded the emission at 381 nm is mainly due to transition $^4D_{3/2} \rightarrow {}^4I_{11/2}$. The contribution of transition $^4D_{7/2} \rightarrow {}^4I_{13/2}$ is negligible.

On the other hand, the 381 nm signal exhibits contributions of both transitions: $^4D_{7/2} \rightarrow {}^4I_{13/2}$ (fast UC signal) and $^4D_{3/2} \rightarrow {}^4I_{11/2}$ (slow UC signal) when the excitation intensity is larger than 30 kW/cm^2. In this case the number of ions excited to level $^4D_{7/2}$ becomes large enough and the amplified spontaneous emission corresponding to transition $^4D_{7/2} \rightarrow {}^4I_{13/2}$ becomes relevant. Therefore, the dynamical behavior of the 381 nm signal is described by $f(t) = A_1 e^{-t/t_1} + A_2 e^{-t/t_2} - A_3 e^{-t/t_3}$, where $A_2 e^{-t/t_2}$ is due to the transition $^4D_{7/2} \rightarrow {}^4I_{13/2}$. The fitting of $f(t)$ to the 381 nm signal for the sample with x = 3.0 is shown of Fig. 5(a) where A_1 = 0.9; A_2 = 19.9; A_3 = 57.9; t_1 = 2.1 μs; t_2 = 0.02 μs; and t_3 = 0.01 μs. The horizontal scale used in Fig. 5(a) allows observing clearly the signal rise time. The inset in Fig. 5(a) shows the fitting for longer times. Figure 5(b) shows the temporal profile of the fast signal component for the sample with x = 3.0, after subtraction of the slow signal component. The inset of the figure shows the signal time behavior at the pumping intensity 20 kW/cm^2. The amplitude of the ≈29 ns pulse is shown in Fig. 5(c) as a function of the pump intensity. The inset in Fig. 5(c) shows the log-log plot of the data. A RL threshold of ≈30 kW/cm^2 can be observed. Notice that by increasing the pump intensity from 20 kW/cm^2 to 55 kW/cm^2 we obtained a 70-fold increase in the emitted intensity at 381 nm.

#142058 - $15.00 USD Received 3 Feb 2011; revised 28 Feb 2011; accepted 28 Feb 2011; published 10 Mar 2011

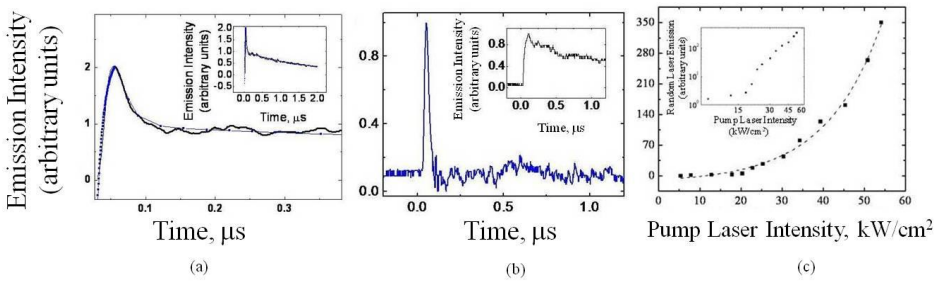

Fig. 5. (a) Temporal behavior of the 318 nm signal for the sample with x = 3.0. Laser intensity: 50 kW/cm^2. The solid blue line represents a fitting of $f(t)$ with the parameters indicated in the text. (b) Temporal behavior of the RL signal (pump intensity: 50 kW/cm^2). The inset shows the signal behavior for pump intensity of 20 kW/cm^2. (c) RL intensity as a function of the laser intensity. Sample: x = 3.0.

In summary, the results presented demonstrate a UC random laser operating in the ultraviolet. The laser is based on the orange-to-ultraviolet conversion obtained in a Nd^{3+} doped fluoride glass powder. The contribution of an energy transfer mechanism for RL generation is reported here for the first time. Considering the large variety known of efficient UC processes involving rare-earth ions the present results show that there is good potential to operate RLs with basis in other UC schemes.

Acknowledgments

We acknowledge the support from the Brazilian Conselho Nacional de Desenvolvimento Científico e Tecnológico (CNPq) through the National Institute of Photonics Project (INCT de Fotônica) and the Fundação de Amparo à Ciência e Tecnologia do Estado de Pernambuco (FACEPE). The Centro de Tecnologias Estratégicas para o Nordeste (CETENE) is acknowledged for electron microscope images.

#142058 - $15.00 USD Received 3 Feb 2011; revised 28 Feb 2011; accepted 28 Feb 2011; published 10 Mar 2011